International Journal of Radiology and Diagnostic Imaging

E-ISSN: 2664-4444
P-ISSN: 2664-4436
www.radiologypaper.com
IJRDI 2024; 7(4): 08-18
Received: 06-08-2024
Accepted: 11-09-2024

Nobukata Kazawa
Department of Radiology, Kansai Medical University, Fumizono, 10-15, Moriguchi, Osaka, Japan

Yuta Shibamoto
Department of Radiology Naogya Cty University, Kawsumi1, Mizuho, Nagoya, Aichi, Japan

Akira Yoshimotoi
Department of Radiology, Kansai Medical University, Fumizono, 10-15, Moriguchi, Osaka, Japan

Tetsuro Sugiura
Department of Cardiology, Kansai Medical University, Fumizono, 10-15, Moriguchi, Osaka, Japan

Satoshi Sawada
Department of Radiology, Kansai Medical University, Fumizono, 10-15, Moriguchi, Osaka, Japan

Noboru Tanigawa
Department of Radiology, Kansai Medical University, Fumizono, 10-15, Moriguchi, Osaka, Japan

Corresponding Author:
Nobukata Kazawa
Department of Radiology, Kansai Medical University, Fumizono, 10-15, Moriguchi, Osaka, Japan

The clinical utility of high resolution 3D-CT in the pleural/pulmonary diseases

Nobukata Kazawa, Yuta Shibamoto, Akira Yoshimotoi, Tetsuro Sugiura, Satoshi Sawada and Noboru Tanigawa

DOI: https://doi.org/10.33545/26644436.2024.v7.i4a.409

Abstract
Objective: To demonstrate the pleuro-pulmonary disease on high resolution 3D image using volume/surface rendering method and multi-collar display segmentation with/without fly-through cross section images.
Materials and Methods: Sixty-one patients (31 men and 30 women; mean 56.6 years old) were examined by thin slice (0.5- 2mm) HRCT, and then the high-resolution 3D volume/surface rendering images were constructed. We compared these HRCT with 3D multi-collar display segmentation with/without fly-through cross section images with conventional volume/surface rendering 3D images.
Results: Visceral pleural involvements by interstitial pneumonia (NSIP, UIP, CVD-IP, CPFE) were clearly displayed. In honeycombing lung or bullous emphysema, the bulging pleural lesions were present and the depression of the pleura by the chest wall or parietal pleural lesions were also demonstrated. The interlobar fissure lines and the inter/peri-lobular septal thickenings were more clearly observed in patients with congestive heart failure or lymphoproliferative disorder compared with conventional CT. The intralobular interstitial thickenings was clearly observed in patients with chronic hypersensitivity pneumonitis, NSIP, and UIP. Conclusion. The detectability rate of pleural lesions, such as visceral pleural lesions in interstitial pneumonia were significantly better on high resolution 3D-CT than the conventional 2D, 3D-CT statistically.

Keywords: Volume rendering CT, Surface rendering CT, HRCT, Pleural lesion, Interstitial pneumonia, Interlobular septal thickening, Intralobular interstitial thickening

Introduction

With innovation of the CT, we have been able to make and appreciate the three/four dimensional images of the human body, such as the vasculature, bronchial tree, and bone in the clinical use1-2,4). Nowadays, we can obtain the volumetric thin slice iso-voxel data more easily and faster with multi-detector (16-64) row CT. HRCT (slice section: 0.5-2 mm) can detect tiny lesions than conventional CT, especially ground- glass opacity(hazy increased attenuation caused by partial filling of air space, interstitial thickening, collapse of alveoli or increased capillary blood volume) and faint emphysema(bullae or lung cyst). Besides axial image, coronal and sagittal reformatted images (multi-plane reconstruction; MPR) would be applied to the radiological diagnosis and monitor the pre-and post-operative status.

We can observe the three-dimensional images from various angles, and make colorful images with the progress of the computer. The 3 DCT applications, such as volume rendering (VR), maximum intensity projection (MIP), and virtual endoscopy have been produced from the last decade. In the field of thoracic radiology, 3D-CT could be easily constructed without use of contrast material because remarkable difference exists in the CT value between the pulmonary vessel/lesion and background air-parenchyma 5-6). Therefore, we can easily recognize the malformation of the pulmonary vessel7), or tracheobronchial anomaly8,9) on the 3D-CT images. The preoperative simulation or intraoperative navigation system with AI have been clinically applied to practice 5). In this article, we introduced the thin slice HRCT images as 3D source images, then we would like to make evolution the 3D-CT images into the new diagnostic tool in various pleural/pulmonary diseases adding multi-collar segmental display accorded with the CT value. We evaluated its clinical utility by radiologic & pathophysiologic correlations and intend to produce the evolutional way of image analysis for the accurate diagnosis.

Table 1: Outline of Pleural/Pulmonary 3DCT Imaging

Classical 3D Imaging Technology
1. Visualization of interlobar fissure [3, 4, 9]
2. 3D-VR or MIP images of bronchial, PA/PV, and bone [5, 6, 7, 12]
3. Virtual bronchoscopy [8]
Evolutional Surface Volume Rendering 3D-CT
- Exhibits subpleural or pleural opacities with or without multi-color display segmentation based on CT value.
1. Intralobular reticulation or pleural involvement by interstitial pneumonia (IP) and/or fibrosis
2. Surface bulging (expansion) caused by bulla and/or honeycombing cyst
3. Depression of pleura by extrapleural lesion (pleural or chest wall tumor) [13]
4. ILS thickening due to congestion, lymphangitis carcinomatosis, or lymphoproliferative disorder (LPD) [9]

The Classical 3D imaging Technology

1. The visualization of interlobar fissure 3, 4, 9)
2. The 3D-VR or MIP images of bronchial, PA/PV, and bone 5, 6, 7, 12)
3. Virtual bronchoscopy 8)

Our evolutional surface volume rendering 3D-CT exhibiting sub/pleural opacities with/without multi-collar display segmentation accorded with the CT value,

1. The intralobular reticulation or pleural involvement by IP and/or fibrosis
2. The surface bulging(expansion) caused by bulla and/or honeycombing cyst
3. The depression of pleura by extrapleural lesion (pleural or chest wall tumor)13)
4. The ILS thickening by congestion、lymphangitis ca. or LPD9)

The 3D-CT arteriography/venography,3D bronchial tree image, virtual bronchoscopy, and 3D-bone surface/volume rendering reconstruction images were clinically used in daily practices1-5). Nowadays, we can obtain the volume data more easily in very short acquisition time with the development of the multi-detector CT (MDCT). Besides axial image, coronal and sagittal reformatted images (multi-plane reconstruction MPR) would be applied to the radiological diagnosis.

Materials and Methods

Sixty-one patients (31 M, 30 F; mean 56.6 years old) with pleural/pulmonary disease were examined by thin slice (0.5-2mm) MDCT, and then the high resolution-3D volume/surface rendering images with multi-collar display segmentation and fly-through cross section images were constructed.

From October 2015 to July 2024,high resolution 3D volume/surface rendering CT images were reconstructed in addition to the convectional 2, 5-5 mm slice 2D-, nad 3D VR images and evaluated in 61 cases(pulmonary emphysema 5、chronic bronchitis 4、lobar pneumonia 4、interstitial pneumonia(idiopathic NSIP4, UIP (IPF) 4, CVD (collagen vascular disease)-related IP6、pleuritis 4、lung cancer 4 (adenocarcinoma 3, squampous carcinoma 1)、atypical mycobacterium infection 6、pleural tumor3(pleural mesothelioma, intercostal schwannoma, pleural dissemination of thymoma)、pneumoconiosis 3、pulmonary sarcoidosis 3、traumatic hemothorax 2、pleuro-parenchymal fibroelastosis(PPFE) 1,chronic hypersensitivity pneumonitis 1, middle lobe syndrome 1 ,left sided heart failure 3, lymphoproliferative disorder 2(MCD ML), lymphangitis carcinomataosa1).We used the 320 ADCT Aquillion one (Toshiba Canon, Tokyo Japan) and 64 row multi detector MDCT; Hi-speed Qxi (GE Medical System, Millwallkey USA) with slice thickness/pitch=0.5-2/0.625-1.25mm and 2.5-5.0/5mm. The other parameters were as follows: 120 kVp, 175-200 mAs, a 25-30 cm field of view, and a 512 × 512 matrix. We acquired the ethics committee approval and the informed consents of all patients. The 3D-CT images were constructed by the advantage window (version 4.1) workstation computer system using volume rendering technique with surface-extracting method. The images were modified with gradated linear opacity curve showing lower density structures than the ground glass opacity. The lower threshold was fixed at－1024HU、and the upper threshold limit was varied at －415+-75HU (-340～-490) in order to avoid the superimposition of the intra-pulmonary structure beneath the lung surface. After removing the chest subcutaneous wall plane manually by the electronic cutting tool, a gray scale display emphasizing the lung visceral surface structure's contrast, and multi-collar display segmentation with/without fly-through cross section images. On the monitor, 3D images were observed at multiple angles with axial, coronal, sagittal 2D reconstructed MPR images.

As a result, faint small lesions could be evaluated more detailed than conventional CT. The volume rendered 3DCT images were inspected mainly from three points. ① Could it depict the fine visceral pleural disease exactly？②Was it able to detect the lung surface bulging lesion, such as emphysematous bullae, honeycombing lung？③Did the linear and polygonal shadows correspond to the interlobar fissure including accessory fissure, and to the interlobular and/or intralobular septal peri-lobular lesions? For those purposes, we reviewed 41 3D VR-CT images with several pleuro-pulmonary diseases at variable angles with axial, coronal, and sagittal 2D reconstructed MPR images. Moreover, we compared the delectability of visceral pleural lesion honeycombing lung bullae/bleb interlobular septal line between 2-2.5/ 5mm slice 2D axial images and high-resolution 3D VR-CT images (Table 1).

We acquired the ethics committee approval and the informed consents of all patients regarding the CT risk and benefits, and the academic use of constituted 3D images 3D workstation systems: AZE Virtual Place and Advantage Window (GE Medical Version 4.1) and AQ net 3D iNtuition (Tera Recon, Inc Version 4.411). The SSR (shaded surface rendering), VR (volume rendering), MIP images, virtual endoscopy and transparent lung parenchymal VR image, multi-collar display segmentation with/without fly-through cross section images have been produced.

The Procedures of 3D Image Construction

With introduction of HRCT, MPR reconstructed high resolution images and 3D-CT can easily recognize the subtle pleural lesions than 2D-CT. The 3D-CT images were constructed by using VR technique with surface-extracting method. Basically,3D images were made using gradated linear opacity curve displaying lower density structures than the lung ground glass opacity. The lower threshold was

fixed at-1024 H.U., and the upper threshold limit was varied at -415+-75Hu (-340～-490) in order to avoid the superimposition of the intra-pulmonary structure beneath the lung surface. After removing the chest wall plane and heart contour by the electronic cutting tool, 3D lung image demarcated by interlobar fissure emerged. The intralobular reticulation, interlobular septum, and visceral pleural tiny opacity(lesion) can be evaluated.

Transparency lung parenchymal VR images were also made by adding consolidation area (-340～-30 H.U.) with/without collaring which highlights abnormal lesion. The multi-collar display segmentation according to the attenuation value was attempted for the discrimination of emphysema/IP/fibrosis/pneumonia or soft tissue tumor from normal lung parenchyma. In some cases, stereoscopic visualization of the internal structure (fly-through internal cross-sectional images) was produced for more precise evaluation. The HRCT can detect more tiny nodules, thin-walled cyst, centrilobular opacities, fine linear structure (ILS) and faint GGO sensitively than conventional CT. Therefore, pleural small dissemination, honeycombing cyst, lymphatic congestion, and interstitial inflammation can be visualized and evaluated on HR (using 0.5-2mm slice)-3DVRCT than ordinal 3D VRCT using 2.5mm collimation images.

By avoiding the superimposition of the lung parenchyma, we can focus on pleura to the subpleural peripheral pulmonary parenchyma. As a result, pleural thickened lesions were clearly demonstrated as high dense opacity even very subtle. Our high resolution 3D volume/surface rendering CT is appreciated to be able to distinguish the visceral pleural thickening from adjacent intercostal muscle, vessels or faint pleural effusion. Moreover, with high resolution 3D volume/surface rendering CT, subpleural lesions such as interstitial pneumonitis (figure1,3) or pleural plaque associated with asbestosis, pleural invasion of bronchogenic carcinoma are more easily to be assessed than only transverse CT. The early detection of the pleural involvement of the lymphoproliferative disorder, pleural dissemination of malignancy is also be anticipated. However there are some limitations; those are ① the outline of the honeycombing lung or bullae were often obscure because of the partial volume effect between the air and the thin wall peripheral lung structure, ② dorsal side lung density were diffusely elevated due to the gravitation effect or incomplete inspiration in some cases

Since faint mediastinal or parietal pleural thickenings were not projected in 3D images, the elevation of the lung surface density represents the visceral pleural lesions fundamentally. Therefore, the discrimination of the visceral and parietal pleura is expected, however when chronic or old inflammatory adhesions exist.

The detectability rate of pleural lesions on 2D (1-2mm thin slice HRCT,5mm slice CT, high resolution 3D- and conventional 3D-VR images were listed as table 1.

Regarding the visceral pleural lesions, significant differences were observed between1-2mm slice and HR3D-VRCT($p < 0.05$), and 5mm slice and 3D-CT($p < 0.01$) statistically (Unpaired Student's t-test)

In the future, intraoperative correlation including MPR, MIP images should also be performed under 3D navigation software10, 11, 12).

By visualizing the lung surface with volume rendering method, pulmonary 3DCT can make some contributions to the clinical radiologic field by the exact detection and assessment of the pleural lesions with high detection rate. We can also observe the lung expansion at a glance. So a functional analysis of the lung expansion in cases of COPD (ex. emphysema) could be expected. Moreover, the distribution and severity can be evaluated in cases of pulmonary edema, or congestion by heart and/or hepatorenal failure by high resolution 3D volume/surface rendering CT. The 3D-CT images were constructed by the advantage window (version 4.1) workstation computer system using volume rendering technique with surface-extracting method. The images were modified with gradated linear opacity curve showing lower density structures than the lung ground glass opacity. The lower threshold was fixed at－1024Hu、and the upper threshold limit was varied at －415+-75Hu (-340～-490) in order to avoid the superimposition of the intra-pulmonary structure beneath the lung surface. After removing the chest wall plane manually by the electronic cutting tool, gray scale display emphasizing the lung surface contrast or colored segmented VR images according to the CT value. On the monitor, 3D VR or MIP images were observed at multiple angles with axial, coronal, sagittal 2D reconstructed MPR images.

As a result, faint small lesions could be evaluated more detailed than conventional CT. The volume rendered 3DCT images were inspected mainly from three points. Could it depict the fine visceral pleural disease exactly？②Was it able to detect the lung surface expansive lesion, such as bullae, honeycombing lung？③Did the linear shadows correspond to the interlobar fissure including accessory fissure, and to the interlobular and/or intralobular septal line thickenings? For those purposes, we reviewed 61 3DVR CT images with several pulmonary diseases at variable angles with axial, coronal, and sagittal 2D reconstructed MPR images. Moreover, we compared the delectability rate of visceral pleura lesion, honeycombing lung, bullae/bleb、interlobular septal line between 2-2.5/ 5mm slice axial images and high-resolution 3D VR CT images (Table 2).

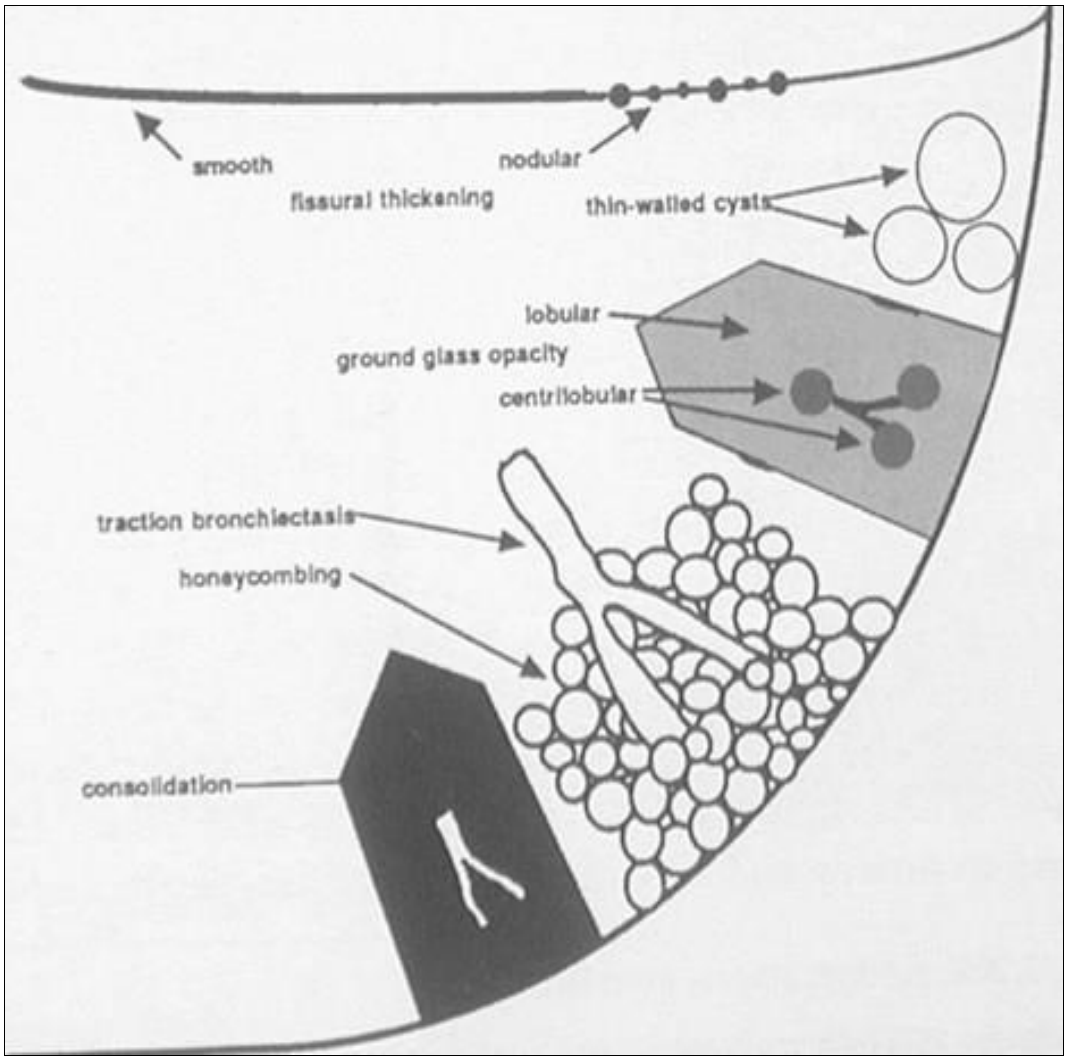

Fig 1: The HRCT can detect tiny nodules, thin walled cyst, centrilobular opacities, fine linear structure(ILS) and faint GGO more sensitively than conventional CT

Table 2: The detectability rate of pleuro-pulmonary lesions on 2DCT (5mm v.s.0.5-2mm thin slice), and 3DVRCT(2.5mm v.s.0.5m HR).N=the number of patients, ()=percentile.

Findings	0.5-2 mm slice	5 mm slice	3D	3D
	HRCT	CT	High resolution VR-CT	VR-CT
Honeycomb Lung	16(19.7)	9(14.8)	13(21.3)	7(11.5)
Plural Indentation	15(24.6)	7(11.5)	16(19.7)	9(14.8)
ILS	20(32.8)	8(13.1)	18(29.5)	11(18.0)
Thickening				
Visceral Pleural Opacity	18(29.5)	7(11.5)	25(40.1)	14(23.0)

The detectability rate of pleural lesions such as, honeycomb lung, plural indentation, I LS thickening, visceral pleural opacity on 2DCT (5mm &0.5-2.mm thin slice), and 3DVRCT(2.5mm &0.5-2mm high resolution source)images were listed. Particularly, visceral pleural lesions in chronic IP were more easily suspected on 3D-VR CT. Regarding the visceral pleural lesions, significant differences were observed between 3DVR and HR-3DVRCT($p < 0.05$), and 5mm slice conventional CT and HRCT($p < 0.01$) statistically.

Results

1. The clinical utility and characteristics of high resolution 3D volume/surface rendering CT

Thanks to the our 3D VR-CT image reflecting lung surface, visceral pleural thickening less than1 mm can be visualized easily. The surface irregularity could also be evaluated, so we can analyze the distribution and severity of the pleural abnormal lesions. However, we could not discriminate the pleura from subpleural lesions discretely on present CT spacial resolution. So, we should take care that a relative high dense surface shadow in the 3D image represents both pleura and subpleural pulmonary lesions.

The distribution and location were precisely correlated between 3D image and the axial, coronal, sagittal MPR images even a faint tiny structure.

With respect to the lesion diagnosis, the detectable rate of lung surface lesions were higher on both HR-3D and conventional pre-existimg3D VR-CT images than respective 2D images (Table 1). Without pleural effusion or pneumothorax, it is very difficult to discriminate the visceral pleura from the parietal pleura on usual CT. However, by

using our 3D model we supposed to have an ability to make discrimination between them. Indeed, ground glass shadows which we think they represent both the pleural and subpleural lesions were more conspicuous than conventional 2D-CT images, although faint increase of the CT density was also caused by gravity dependent effect or incomplete inspiration particularly in the dorsal lung fields.

Soft tissue density mass involving the chest wall or alveolar pneumonia reaching the pleura were displayed as a pleural defect、pleural indentation and pleural tag caused by lung cancer were depicted as a thin linear opacity or the complex of several convergences of the visceral pleura.

2. Pleural density

In cases of interstitial pneumonia, many ground glass with reticulation and/or fine dot opacities were observed in the lung surface. Subpleural inflammatory changes, such as fibrous thickening or visceral pleural involvement were clearly observed even very subtle. So, all faint pleural changes were observed as relatively high density shadows besides lower lobe basal area (fig. 2, 3, 6).

By the MPR image correlations, superficial smoothly depressed area precisely corresponded to the thickening of the visceral pleura and subpleural lesions(Figure2a,b). The small nodular dot-like shadows scattering the plural surface were correlated with the dilatation of the peripheral lung vessels or thickening of interlobular septum. Concerning the dependent ground glass opacity in the dorsal lung field, not only (sub)pleural lesion shadows but also partial volume effect, such as the gravitation effect were associated. There are possibilities that their high density areas are due to the increase of blood perfusion or peripheral lung collapse. The faint linear to irregular band shadows were assumed to be formed by the irregular thickening of the pleura, subpleural fibrosis(Fig, 2, 3) and collapse of the alveoli (Fig.3, 6)

Regarding the visceral pleural lesions, significant differences were observed between 0.5-2mm slice HRCT and 3DCT($p = 0.0276 < 0.05$), and 5mm slice and 3DCT($p = 0.0087 < 0.01$) statistically(Unpaired Student's t-test)

Fig 2. Chronic interstitial pneumonitis (f NSIP pattern) fibrotic interstitial pneumonitis with fine honeycombing lung

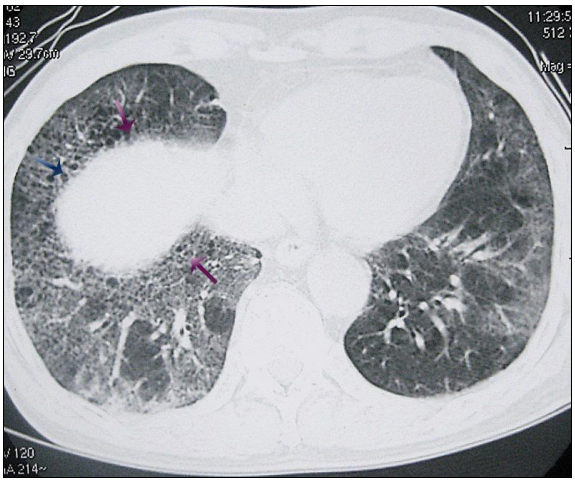

Fig 2a: axial lung base CT at the costophrenic angel level

We can observe diffuse ground glass opacities and the microscopic honeycombing cysts(arrows) caused by subpleural fibrosis in both lower lung fields.

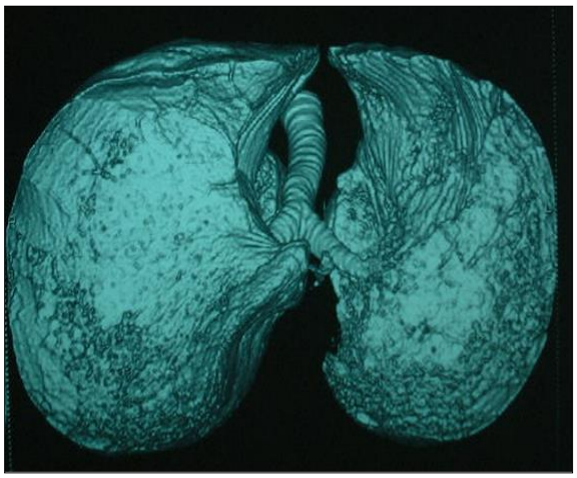

Fig 2b: 3 D-high resolution VRCT lung base view.

Especially, we can observe the honecycombing lung(arrows) with hobnail appearance. We can observe the patchy ground glass and reticular opacities reflecting the chronic interstitial inflammation projecting on the surface of the both lung.

Fig 3. RA lung and MPO-ANCA related UIP presenting SCLS (bridging collapse/fibrosis) with coarse cystic change can be clearly visualized as light green collared area on cross-section image of HR 3D-VRCT.

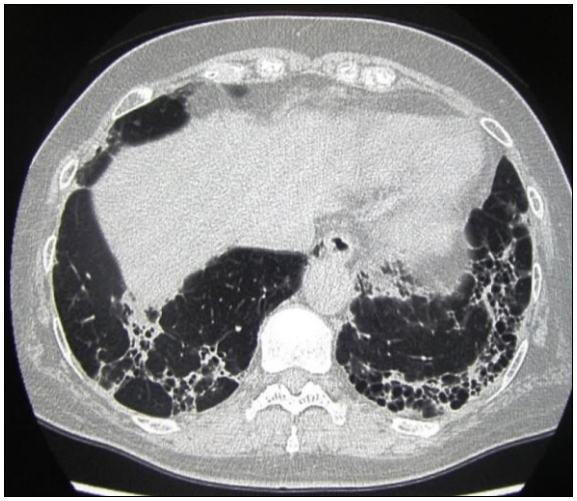

Fig 3a:1mm HRCT 3

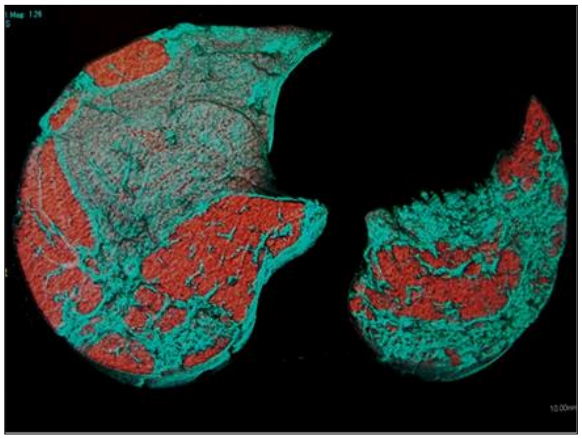

Fig 3b: The cross-section image of the HR 3D-VRCT

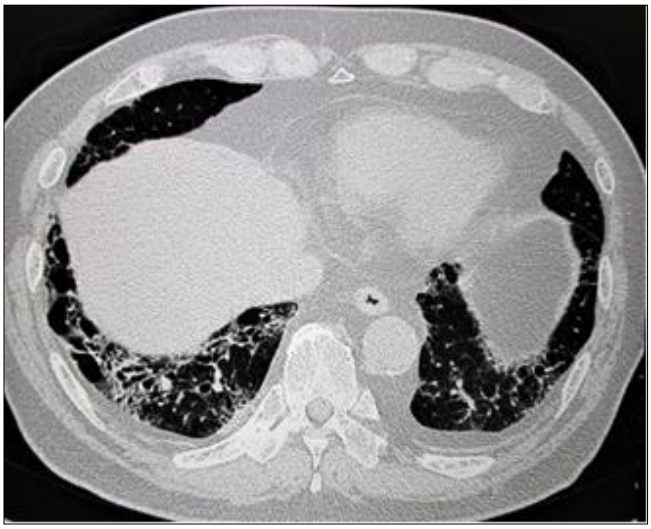

Fig 4a: In a 70y.o.Fe

Fig 4b: Segmented VR(volume rendering) image

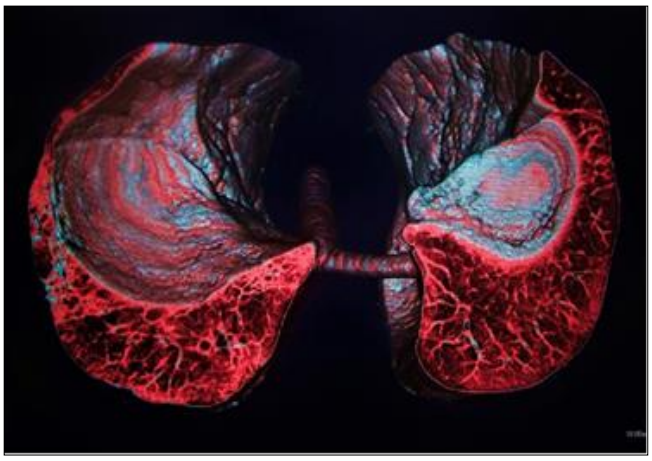

Fig 4c: Cross-section image of HR 3D-VRCT

The lower lobe dominant subpleural IP has worsened and the volume loss due to the collapse of alveoli have progressed.

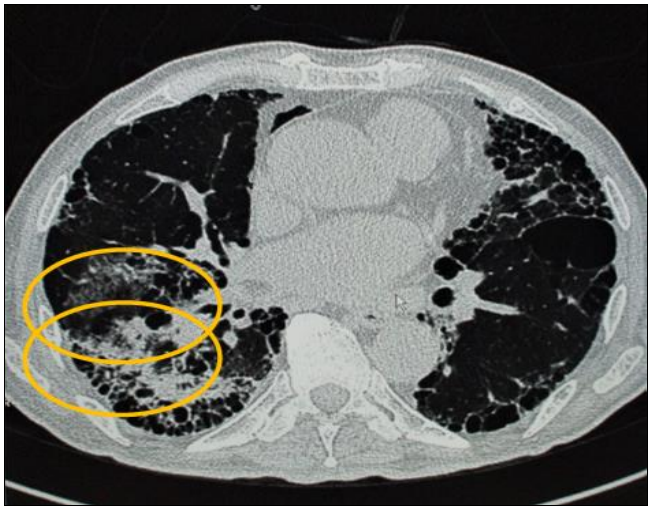

Fig 5a: CPFE &Air-space Consolidation.

In a -56-year-old man. case, bacterial pneumonia was superimposed simultaneously (WBC8200 CRP5.94).The several alveolar filling consolidations with air-bronchogram (yellow circles) and pneumomediastinum(arrow) were stereoscopically observed on fly-through coronal sections

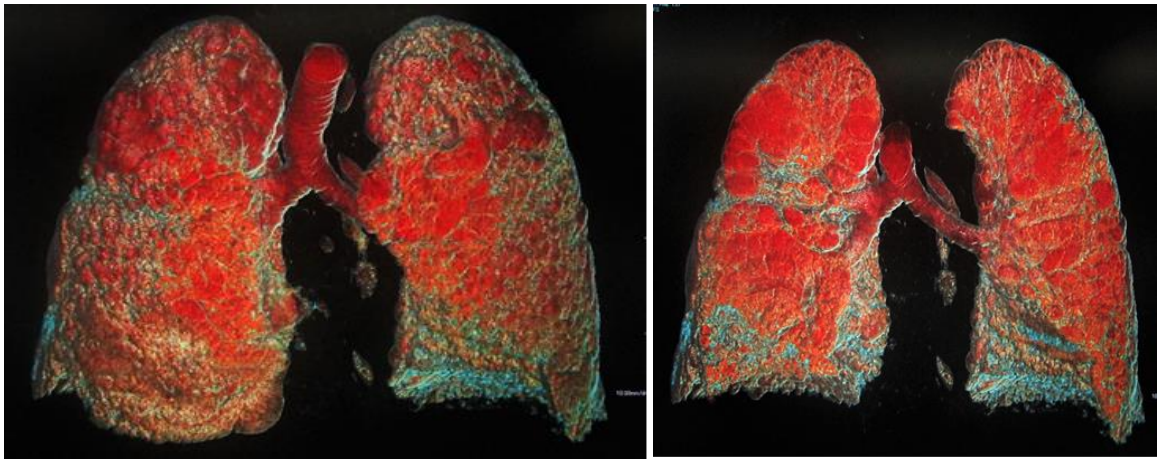

Fig 5b, c: 3D- high resolution VRCT lung

Bacterial infective pneumonia was superimposed simultaneously (WBC8200 CRP5.94). The several alveolar filling consolidations with air-bronchogram () were stereoscopically observed on fly-through coronal sections; On transaxial CT, subpleural curvelinear opacities with small nodular pleural thickening were observed in the left lower lobe(arrows). They distributed trans segmentally.
Figure 6 Traumatic Lung Contusion in a-18-year old female fallen off during horse riding exercise.

Fig 6a: On transaxial CT, subpleural curvilinear opacities with small nodular pleural thickenings were observed in the left lower lobe(arrows). They distributed trans-segmentally along the pleura.

Fig 6b: The posterior view of the 3D- high resolution VR CT. We can observe the patchy high dense opacities(arrows) projecting on the surface of the lt. posterior pleural plane which suggests subpleural alveolar collapse and/or visceral pleura lesion (damage).

Figure 7 The pulmonary edema in the congestive heart failure in a 76-year-old man.

Trans-axial CT: We can observe so-called the "Kerley Lines" (arrows) Pulmonary Edema in the Congestive Heart failure in a-76-y.o.M.

The high resolution 3D volume/surface rendering CT; the frontal oblique view. We can observe so called the kerley lines (arrows) in the left lingular lobe with bilateral medium amount of pleural effusion. On 3D-VRCT, the polygonal thickening of the smooth interlobular septum are clearly visualized on the lingular lobe edge （white circle） which represents the edematous interstitium.

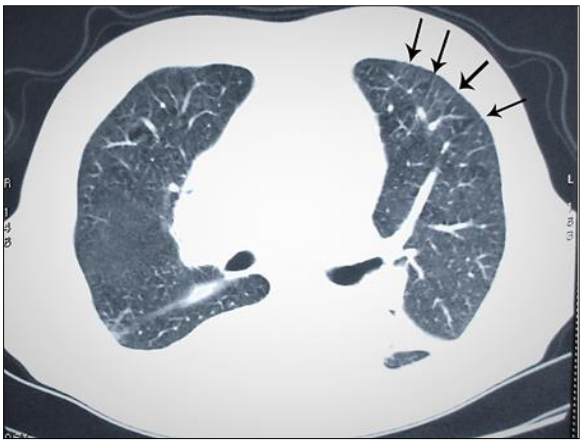

Fig 7a: Transaxial CT. We can observe so called the kerley lines (arrows)

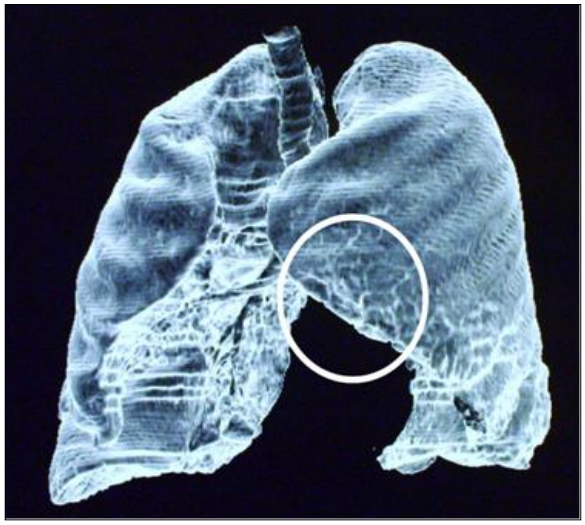

Fig 7b: The high resolution 3D volume/surface rendering CT, the frontal view lung

We can observe so called the kerley lines (arrows) in the left lingular lobe with rt. medium amount of pleural effusion. On 3D VR-CT ,the polygonal thickening of the the interlobular septum are clearly visualized on the lingular lobe edge （white circle）which represents the edematous interstitial thickening.

3. Linear structures on pleural surface

The interlobar fissure or accessory fissure such as left minor fissure, azygos lobe fissure were depicted nicely on high resolution 3D VR-CT. And the continuation and localization were more clearly evaluated than conventional 2D CT. The displacement or shift of the interlobar fissure caused by the hemi-agenesis of the lung or lobar atelectasis were clearly visualized. The intralobular intersrtitial thickening were observed in a patient of hypersensitivity pneumonitis. The thickening of the interlobular septum like the turtle shell were observed in cases of pulmonary sarcoidosis, or congestive heart failure (Fig.7,) lymphoproriferative disease severity and distribution could be evaluated by viewing form the multiple angles.

The detectability rate of pleural lesions on 2D(0.5-2mm thin slice)CT,5mm slice CT, and high resolution 3D-VR CT, conventional 3D-CT images were listed as table 2. Regarding the sensitivity of the linear shadows, both conventional CT and 3D VR-CT were almost same outcome, however, the distribution of the interstitial spread of abnormal cell were more obvious in high resolution 3D-VR CT.

Discussion

Three dimensional CT has been introduced to the clinical field of diagnostic chest radiology since helical (spiral) CT has been applied to practice 1,2). Mainly its clinical use was applied in simulation and navigation for bronchoscopy or VATS or robotic surgery by visualization of the airway and pulmonary vessel and mediastinal anatomy, and/or screening of rib fracture and bone tumor 7-11).

Due to the evolution of the multi-detector row CT(MDCT), the improvement of the image resolution and reduction of the motion artifact have been achieved 3,4,5). By setting the upper threshold density to－415±75(—340～—490)HU which was the attenuation of lung ground glass inflammation, we could focus and evaluate the abnormal lesions of the pleura and the subpleural peripheral pulmonary parenchyma.

By avoiding the overlap of the lung parenchyma, we focused the abnormal lesions of the pleura and peripheral pulmonary parenchyma especially on 3D-VR (SSR)CT. As a result, faint pleural thickenings were clearly demonstrated as high dense opacity even if very subtle. Then, transparency lung parenchymal VR images were also made by adding consolidation area(-30～-340H.U.)

With collaring highlighting abnormal opacities by widening the opacity transparency.

The multi-collar display segmentation in accordance with CT value(number) was attempted for the discrimination of emphysema(<-950)/IP(<-340)/fibrosis(<- 00)/pneumonia(<-30)or soft tissue(<60H.U.) from normal lung.

The interlobar fissure or accessory fissure such as left minor fissure, and azygos fissure were nicely depicted（Fig.7). The displacement or shift of the interlobar fissure caused by the hemi-agenesis of the lung or lobar atelectasis were also clearly visualized.

4. In our 3D model, ground-glass, and reticular opacities which we think they represent both the pleural and subpleural lesions were conspicuous than 2D images. Concerning the dependent opacity in the dorsal lung field, not only (sub)pleural lesion but also partial volume effect, such as the gravitation effect was associated. Other possible causes of high opacities are the increase of blood perfusion(congestion) or peripheral lung collapse. The faint linear to irregular band shadows were assumed to be formed by the irregular thickening of the pleura, subpleural fibrosis (Fig.4-7), and collapse of the alveoli (Fig.3). The intralobular interstitial thickenings were observed in patients.

New high resolution 3D volume/surface rendering CT made by thin slice (0.5-2.0 mm)images is expected to be capable to distinguish the visceral pleural thickening from adjacent intercostal muscle, vessels or faint pleural effusion expanding the window width. Moreover, high resolution 3D volume/surface rendering CT, the subpleural lesions such as interstitial pneumonia (Fig2,3) or traumatic lung surface contusion(Fig 6),pleural plaque associated with asbestosis, pleural invasion of bronchogenic carcinoma,and subplerual fibrosis of PPFE were more easily to be assessed than conventional 3D-CT images. The early detection of the pleural involvement of the lymphoproliferative disorder, pleural dissemination of malignancy are also anticipated. However there are some limitations; those are ①the outline of the honeycombing lung or bullae were often obscure because of the partial volume effect between the air and the thin wall peripheral lung structure, ②dorsal sided lung opacity were diffusely elevated due to the gravitation effect, congestion edema and/or incomplete inspiration in some cases.

The detectability rate of pleural lesions on 2D(0.5-2mm thin slice HR,5mm slice CT, and high resolution and pre-existing conventional 3D-VR images were compared as table 1. Regarding the visceral pleural lesions, significant differences were observed between 3DVR and HR-3DVRCT($p < 0.05$), and 5mm slice conventional CT and HRCT($p < 0.01$)s tatistically. The detection of faint bullous lesion on HR-3DVR was slightly higher than HRCT or 3DVRCT ($p<0.05$) (Unpaired Student's t-test).

By visualizing the lung surface with volume rendering method, pulmonary 3D VR-CT can make some contributions to the clinical radiologic field by the exact detection and assessment of the pleural lesions with high detection rate. We can also observe the lung expansion at a glance. So a functional analysis of the lung expansion during respiration in cases of COPD (e.g. emphysema) would be performed soon.

On both thin-slice HRCT and 3D VR-CT, faint interstitial lesions showing intra/interlobular septal thickenings were observed in congestive heart failure and lymphoproliferative diseases.

Moreover, the distribution and the severity can be evaluated more easily in cases of pulmonary edema, or pulmonary congestion by heart and/or hepatorenal failure on the high-resolution 3D volume/surface rendering CT.

Limitations and Perspectives

The limitations of this study were as follows1) the CT machine and the scanned parameters (slice thickness/pitch=0.5-2/0.625-2.5mm) were not uniform and,

2) the number of subjects was not large. So the radiologic-pathological correlations were not done in all cases. In the future, the quantitative evaluation such as volume estimation of the abnormal lesions would be demonstrated.
The opacity of lung base areas or dorsal subpleural area at times elevate slightly due to the gravitation effect, congestive interstitial edema, incomplete inspiration, the increase of the lung surface density represents the visceral pleural lesions fundamentally because faint mediastinal or parietal pleural thickenings were not projected on 3D VR images. Therefore, the discrimination of the visceral and parietal pleura is expected unless chronic or old inflammatory adhesions exist.

Conclusion
The high resolution 3D-VR (Three Dimensional Volume/shaded surface rendering) CT and transparency lung parenchymal VR CT image, multi-collar display segmentation with/without fly-through cross section images of 61patients were displayed and analyzed. Visceral pleural lesions of the interstitial pneumonia (NSIP, UIP, CPFE, CVD-IP) and lung contusion were clearly displayed.
In bullous emphysema and honeycombing lung, inflative pleural plane was observed. The depression of pleural surface was also present by the chest wall or parietal pleural lesions such as pleural plaque, PPFE or extra lung tumor. Interlobar fissure lines were more clearly seen compared with conventional axial CT images. The intralobular abnormal structure thickenings were also clearly observed in patients with interstitial inflammation such as hypersensitivity pneumonitis, congestive heart failure and lymphoproliferative diseases. The interlobular septal thickenings was observed in congestive heart failure, sarcoidosis and lymphangitis carcinomatosa. The sensitivity of subtle pleural lesions on HR 3D-VRCT was significantly better than the conventional 3D-CT had a much high sensitivity than conventional 2D-CT statistically.

Abbreviations
- **HRCT: High Resolution Computed Tomography**
- **IP:** interstitial pneumonia
- **NSIP: Non-Specific** interstitial pneumonia
- **UIP: Usual** interstitial pneumonia
- **CVD-IP: Collagen vascular disease-** interstitial pneumonia
- **CPFE: Combined pulmonary fibrosis and emphysema**
- **PA: Pulmonary artery**
- **PV: Pulmonary vein**
- **MCD:** Multicentric castleman disease
- **ML:** Malignant lymphoma
- **ADCT:** Area detector CT
- **MDCT:** Multi detector CT

Acknowledgement
Not available.

Author's Contribution
Not available.

Conflict of Interest
Not available.

Financial Support
Not available.

References
1. Vock P, *et al*. Lung: spiral volumetric CT with single-breath-hold technique. Radiology. 1990;176:864-867.
2. Remy J, *et al*. Multiplanar and three-dimensional reconstruction techniques in CT: impact on chest diseases. Eur Radiol. 1998;8:335-355.
3. Suzuki N. The fundamental of the three-dimensional medial image technology. Japan Clinical Radiology. 1996;41:1166-1177.
4. Drebine RA. Volume rendering. Computer Graphics. 1988;22:65-74.
5. Fukuhara K, *et al*. Preoperative assessment of the pulmonary artery by three-dimensional computed tomography before video-assisted thoracic surgery lobectomy. Eur J Cardiothorac Surg. 2008;34:875-877.
6. Kuriyama K, *et al*. Pleural invasion by peripheral bronchogenic carcinoma: assessment with three-dimensional helical CT. Radiology. 1994;191:365-369.
7. Rankin S, *et al*. CT diagnosis of pulmonary arteriovenous malformations. J Comput Assist Tomogr. 1982;6:746-749.
8. Fleiter T, *et al*. Comparison of real-time virtual and fiberoptic bronchoscopy in patients with bronchial carcinoma: opportunities and limitations. AJR. 1997;169:1591-1595.
9. Koletsis EN, *et al*. Tumoral and non-tumoral trachea stenosis: evaluation with three-dimensional CT and virtual bronchoscopy. J Cardiothorac Surg. 2007;12:2-18.
10. Kazawa N, *et al*. HRCT images of pulmonary cryptococcosis: the radiologic pathological correlations in 10 cases. Japanese Journal of Clinical Radiology. 2001;46:80-88.
11. El-Solh AA, *et al*. Clinical and radiographic manifestations of uncommon pulmonary nontuberculous mycobacterial disease in AIDS patients. Chest. 1998;114:138-145.
12. Kawamoto S, *et al*. Three-dimensional CT angiography of the thorax: clinical applications. Semin Ultrasound CT MR. 1998;19:425-438.
13. Oizumi H, *et al*. Lung surgery assisted by multidetector-row computed tomography simulation. Jpn J Chest Surg. 2009;23:912-917.
14. Iwasawa T, *et al*. The importance of subpleural fibrosis in the prognosis of patients with idiopathic interstitial pneumonias. Eur J Radiol. 2017;90:106-113.
15. Vanessa A, *et al*. High-resolution multidetector CT-aided tissue analysis and quantification of lung fibrosis. Acad Radiol. 2007;14:772-787.
16. Ra Gyoung Y, *et al*. Quantitative assessment of change in regional disease patterns on serial HRCT of fibrotic interstitial pneumonia with texture-based automated quantification system. Eur Radiol. 2013;23:692-701.
17. Panayiotis DK, *et al*. Vessel tree segmentation in the presence of interstitial lung disease in MDCT. IEEE Trans Inf Technol Biomed. 2011;15(2):214-220.
18. Uchiyama Y, *et al*. Quantitative computerized analysis of diffuse lung disease in high-resolution computed tomography. Med Phys. 2003;30:2440-2454.
19. Iwao Y, *et al*. Integrated lung field segmentation of injured region with anatomical structure analysis by

failure-recovery algorithm from chest CT images. Biomed Signal Process Control. 2014;12:28-38.

How to Cite This Article
Kazawa N, Shibamoto Y, Yoshimotoi A, Sugiura T, Sawada S, Tanigawa N, *et al*. The clinical utility of high resolution 3D-CT in the pleural/pulmonary diseases. International Journal of Radiology and Diagnostic Imaging. 2024;7(4):08-18.